A peer-reviewed version of this preprint was published in PeerJ on 4 January 2016.

View the peer-reviewed version (peerj.com/articles/1543), which is the preferred citable publication unless you specifically need to cite this preprint.

Yoshioka S, Newell PD. 2016. Disruption of *de novo* purine biosynthesis in *Pseudomonas fluorescens* Pf0-1 leads to reduced biofilm formation and a reduction in cell size of surface-attached but not planktonic cells. PeerJ 4:e1543 https://doi.org/10.7717/peerj.1543

Disruption of *de novo* purine biosynthesis in *Pseudomonas fluorescens* Pf0-1 leads to reduced biofilm formation and a reduction in cell size of surface-attached but not planktonic cells

Shiro Yoshioka, Peter D Newell

Pseudomonas fluorescens Pf0-1 is one of the model organisms for biofilm research. Our previous transposon mutagenesis study suggested a requirement for the *de novo* purine nucleotide biosynthesis pathway for biofilm formation by this organism. This study was performed to verify that observation and investigate the basis for the defects in biofilm formation shown by purine biosynthesis mutants. Constructing deletion mutations in 8 genes in this pathway, we found that they all showed reductions in biofilm formation that could be partly or completely restored by nucleotide supplementation or genetic complementation. We demonstrated that, despite a reduction in biofilm formation, more viable mutant cells were recovered from the surface-attached population than from the planktonic phase under conditions of purine deprivation. Analyses using scanning electron microscopy revealed that the surface-attached mutant cells were 25~30% shorter in length than WT, which partly explains the reduced biomass in the mutant biofilms. The laser diffraction particle analyses confirmed this finding, and further indicated that the WT biofilm cells were smaller than their planktonic counterparts. The defects in biofilm formation and reductions in cell size shown by the mutants were fully recovered upon adenine or hypoxanthine supplementation, indicating that the purine shortages caused reductions in cell size. Our results are consistent with surface attachment serving as a survival strategy during nutrient deprivation, and indicate that changes in the cell size may be a natural response of *P. fluorescens* to growth on a surface. Finally, cell sizes in WT biofilms became slightly smaller in the presence of exogenous adenine than in its absence. Our findings suggest that purine nucleotides or related metabolites may influence the regulation of cell size in this bacterium.

Disruption of *de novo* purine biosynthesis in *Pseudomonas fluorescens* Pf0-1 leads to reduced biofilm formation and a reduction in cell size of surface-attached but not planktonic cells

Shiro Yoshioka[1,*] and Peter D. Newell[2]

[1]Institute for Molecular Science, National Institutes of Natural Sciences, 5-1, Higashiyama, Myodaiji, Okazaki, Aichi 444-8787 Japan
[2]Department of Biological Sciences, Oswego State University of New York, Oswego, New York 13126 USA

*Corresponding author
Shiro Yoshioka
Institute for Molecular Science, National Institutes of Natural Sciences,
5-1, Higashiyama, Myodaiji, Okazaki, Aichi 444-8787 Japan
E-mail: yoshioka@ims.ac.jp
TEL: +81-564-59-5577
FAX: +81-564-59-5576

Key Words: *de novo* purine nucleotide biosynthesis, biofilm, cell size, nutrient deprivation

Abstract

Pseudomonas fluorescens Pf0-1 is one of the model organisms for biofilm research. Our previous transposon mutagenesis study suggested a requirement for the *de novo* purine nucleotide biosynthesis pathway for biofilm formation by this organism. This study was performed to verify that observation and investigate the basis for the defects in biofilm formation shown by purine biosynthesis mutants. Constructing deletion mutations in 8 genes in this pathway, we found that they all showed reductions in biofilm formation that could be partly or completely restored by nucleotide supplementation or genetic complementation. We demonstrated that, despite a reduction in biofilm formation, more viable mutant cells were recovered from the surface-attached population than from the planktonic phase under conditions of purine deprivation. Analyses using scanning electron microscopy revealed that the surface-attached mutant cells were 25~30% shorter in length than WT, which partly explains the reduced biomass in the mutant biofilms. The laser diffraction particle analyses confirmed this finding, and further indicated that the WT biofilm cells were smaller than their planktonic counterparts. The defects in biofilm formation and reductions in cell size shown by the mutants were fully recovered upon adenine or hypoxanthine supplementation, indicating that the purine shortages caused reductions in cell size. Our results are consistent with surface attachment serving as a survival strategy during nutrient deprivation, and indicate that changes in the cell size may be a natural response of *P. fluorescens* to growth on a surface. Finally, cell sizes in WT biofilms became slightly smaller in the presence of exogenous adenine than in its absence. Our findings suggest that purine nucleotides or related metabolites may influence the regulation of cell size in this bacterium.

PeerJ PrePrints | https://dx.doi.org/10.7287/peerj.preprints.1307v1 | CC-BY 4.0 Open Access | rec: 13 Aug 2015, publ: 13 Aug 2015

Introduction

ATP and GTP are the purine nucleotide triphosphates that are essential to drive many cellular processes in all living organisms. ADP and GDP are utilized as DNA precursors after being converted to the deoxy forms by ribonucleotide reductase (Neuhard and Nygaard, 1987). AMP and GMP are the dephosphorylated forms of the above nucleotides and synthesized either in a *de novo* synthesis pathway or in a salvage pathway (Neuhard and Nygaard, 1987). In the *de novo* purine biosynthesis pathway, inosine monophosphate (IMP) is sequentially synthesized from 5-phosphoribosyl-α-diphospahte (PRPP) in 11 enzymatic steps, where some reactions require ATP to proceed. AMP and GMP are synthesized separately from IMP as the common intermediate. Therefore, the biosynthesis of purine nucleotides has a high energy cost. For this reason, another biosynthesis pathway, salvage pathway, is designed to scavenge and recycle the purine bases arising from nucleic acid turnover; adenine, guanine, and hypoxanthine are converted into AMP, GMP and IMP, respectively, by phosphoribosyltransferases (Neuhard and Nygaard, 1987). The fact that most bacteria possess both *de novo* purine biosynthesis pathway and salvage pathway indicates vital role of this pathway in bacteria.

The importance of the *de novo* purine biosynthesis in bacterial growth has been repeatedly described in the literature. If one of the genes in *de novo* purine biosynthesis pathway is disrupted, the mutant becomes purine auxotroph. In other words, the mutant is not able to grow unless the exogenous purine bases such as adenine and hypoxanthine are supplied. Purine requiring mutants of some pathogenic bacteria have been found to be avirulent in murine models of infection, implying that the purine requiring mutants stop growing when exogenous purines are not available at the sites of infection, leading to attenuated infection (Bacon, Burrows & Yates, 1951; Gerber, Hackett & Franklin, 1952; Straley & Harmon, 1984; Wang et al, 1996; Polissi et al., 1998; Pilatz et al., 2006; Samant et al., 2008; Jenkins et al., 2011). Furthermore, recent research has highlighted the role of the purine nucleotide biosynthesis on

PeerJ PrePrints | https://dx.doi.org/10.7287/peerj.preprints.1307v1 | CC-BY 4.0 Open Access | rec: 13 Aug 2015, publ: 13 Aug 2015

biofilm formation and symbiosis with nematode, insect or plant roots (Han et al., 2006; Ge et al., 2008; An and Grewal, 2011; Kim et al., 2014a). In these studies, significant reductions in biofilm formation and defects in symbiotic ability were observed for the purine auxotrophic mutants, emphasizing important roles of the purine biosynthesis pathway in biofilm formation and symbiosis (Han et al., 2006; An and Grewal, 2011; Ge et al., 2008; Kim et al., 2014a).

The purine nucleotide derivative c-di-GMP is a central player in the regulation of biofilm formation. Generally, increase in cellular level of c-di-GMP facilitates biofilm formation. This compound is synthesized from two molecules of GTP by diguanylate cyclases (DGCs) possessing GGDEF domain (Paul et al., 2004; Ryjenkov et al., 2005), and degraded by phosphodiesterases (PDEs) containing either EAL or HD-GYP domain (Christen et al., 2005; Schmidt, Ryjenkov & Gomersky, 2005; Ryan et al., 2006). As these enzymes typically contain regulatory domains, the synthesis and degradation of c-di-GMP is influenced by environmental factors.

While DGCs and PDEs have the primary role in controlling the c-di-GMP level, previous work suggested that nucleotide pools impact c-di-GMP levels (Monds et al., 2010; Kim et al., 2014b). The disruption of the *purT* gene in the *de novo* purine biosynthesis pathway decreased cellular concentration of c-di-GMP, leading to defect in the biofilm formation by *Burkholderia* species (Kim et al., 2014b). Increase in c-di-GMP level was observed for the *apaH* mutant of *Psudomonas fluorescens* Pf0-1, which is caused by promotion of the *de novo* purine biosynthesis through increased level of di-adenosine tetraphosphate (Ap4A) (Monds et al., 2010). As for the purine auxotrophic mutants of *P. fluorescens*, biofilm formation could be impaired because the cellular concentrations of c-di-GMP may be decreased due to a reduced pool of GTP.

P. fluorescens Pf0-1 is a soil bacterium that promotes plant growth by forming biofilms on roots (Haas and Defago, 2005). This bacterium forms a biofilm using LapA, a large cell-surface adhesion protein with a molecular weight of ~520kDa (Hinsa et al., 2003). The secretion and localization of LapA is

regulated by LapD that binds c-di-GMP (Monds et al., 2007; Newell, Monds & O'Toole, 2009). To identify the DGC genes involved in biofilm formation by this bacterium, we previously performed transposon mutagenesis and found that more than 50 genes are involved in the biofilm formation (Newell et al., 2011b). Among the mutants impaired in biofilm formation, the transposon insertions occurred in the *purH*, *purL*, *purM*, *purF*, and *purK* genes in *de novo* purine nucleotide biosynthesis pathway (Table S3 in Newell et al., 2011b). We therefore hypothesized that the *de novo* purine biosynthesis pathway is essential for the biofilm formation by this bacterium, as reported for other bacteria.

In this study, we sought to determine the basis for the biofilm formation defects observed in these mutants. To verify the requirement of the purine biosynthesis genes in biofilm formation, we constructed clean deletion mutants and performed functional complementation with exogenous genes and purine bases. Using electron scanning microscopy and a laser diffraction particle analyzer, we demonstrate that the surface-attached cells have smaller cell size compared to the planktonic cells and that the biofilm cells for the purine-depleted mutants became smaller than the WT cells. These data suggest purine auxotrophs of *P. fluorescens* are capable of surface attachment, but produce less biofilm biomass due to the impact of purine deprivation on growth and cell size.

Materials & Methods

Strains and media. Strain SMC4798 was used as the wild-type (WT) *P. fluorescens* Pf0-1, which expresses fully functional three-hemagglutinin (HA)-tagged LapA (Monds et al., 2007; Newell, Monds, & O'Toole, 2009; Newell et al., 2011b; Boyd et al., 2014). *Escherichia coli* S17-1 (λpir) was used for cloning and conjugation. *P. fluorescens* and *E. coli* were routinely cultured with LB medium in a test tube or on a solidified LB medium with 1.5 % agar at 30°C and 37°C, respectively. *Saccharomyces cerevisiae* strain InvSc1 (Life Technologies) was used to construct plasmids for clean deletion and complementation, as previously described (Shanks et al., 2006). Gentamycin (Gm) was used at 30 μg/ml for *P. fluorescens* and at 10 μg/ml for *E. coli*. Chloramphenicol (Cm) was used at 30mg/ml. For biofilm assay, K10T-1 medium that has been used in this laboratory and consisted of 50mM Tris-HCl (pH 7.4), 0.2% Bacto tryptone, 0.15% glycerol, 0.61mM $MgSO_4$, and 1mM K_2HPO_4, was used (Monds et al., 2006). Purine bases were added to K10T-1 to a final concentration of 0.2mM. Arabinose was used to induce expression of the P_{BAD} promoter from pMQ72 vector at a final concentration of 0.1% (wt/vol).

Biofilm formation assay. Biofilm formation assays were performed using a polyvinyl chloride 96-well round-bottom microtiter plate (Corning 2797). Aliquots (1.5μl) of liquid cultures grown overnight in LB medium was added to 100μl of K10T-1 medium in the microtiter plate, and statically incubated at 30°C for 6hrs. After incubation, the liquid cultures were discarded, and the biofilm cells were stained with 0.1% (wt/vol) crystal violet (CV) in water. Twenty minutes later, the microtiter plates was rinsed with water three times, and air dried. Quantification of the biofilm cells was performed as previously described (Monds et al., 2007). In brief, 150μl of 30% acetic acid (vol/vol) was added to the microtiter plate to solubilize the CV, and 125μl of this solution was transferred into a flat-bottom microtiter plate. A microplate reader Vmax (Molecular Devices) was used to read the absorbance at 550nm.

Constructs for clean deletion and complementation. The pMQ30

and pMQ72 vectors were used for clean deletion and complementation, respectively. Clean deletion mutants were prepared as follows. A ~1kbp pair of PCR fragments was amplified from upstream and downstream of the target genes. The fragments were cloned into pMQ30 in parallel. Deletion constructs were transferred into *P. fluorescens* by conjugation, and transconjugates were selected on LB plates containing Gm and Cm. After confirming the single-crossover events by PCR, the strains were cultured overnight in the absence of any antibiotics and then spread on LB medium agar plate containing 5% (wt/vol) sucrose to facilitate the second crossover recombination. The removals of the target genes were verified by PCR, and all mutants resulted in the reduced biofilm in the biofilm formation assay. The pMQ72 vectors for complementation were designed to possess the ribosomal binding site (RBS) for LapD (Newell, Monds & O'Toole, 2009) and the N-terminal 6× histidine (6×His) tag. Success in construction was confirmed by DNA sequencing. The pMQ72 vectors were introduced into the *P. fluorescens* strains by electroporation.

Measurement of numbers of planktonic and biofilm cells. Number of cells in the supernatants and biofilms were determined by a serial dilution method. After incubation for biofilm assay, the supernatants were removed, and the wells were washed twice with 100μl of PBS buffer consisting of 10mM Na_2HPO_4, 2mM KH_2PO_4, 137mM NaCl, and 2.7mM KCl. An aliquot (100μl) of the PBS buffer was added to the wells, and the biofilm cells were collected using a disposal cotton swab (Shimada et al., 2012). The cotton swab was then put into an Eppendorf tube, and the well was washed twice with 100μl of the PBS buffer. The washed buffers were transferred into the Eppendorf tube each time. After adjusted to 1mL, the solution was vigorously vortexed and used for the serial dilution to determine the numbers of the cells. Successful removal of the biofilm cells from the wells was confirmed by staining the microtiter plates with CV, where the residual stain was negligible for all cases.

Scanning electron microscopy. Scanning electron micrographs were obtained for the biofilms formed inside the 96-well microtiter plate, followed by

platinum ion sputtering (MSP-1 magnetron sputter, Vacuum Device Inc., Japan). A desktop scanning electron microscopy Phenom ProX (Phenom World, The Netherlands) was employed with the accelerating voltage of 10kV. To obtain information on cell size, the electron micrographs were analyzed using Phenom ParticleMetric software (Phenom World, The Netherlands). From each micrograph, single cells were identified and parameters such as circumscribed circle diameter and circle equivalent diameter were automatically obtained. The circumscribed circle diameters for more than 1,000 cells were utilized to make the histograms for each strain.

Laser diffraction particle analysis. Size distributions of the planktonic and biofilm cells were measured using a laser diffraction particle analyzer LA-960 (Horiba, Japan). Particle size analysis was performed with the software equipped with the device. In this analysis, the software calculates the size of particles based on the Mie theory, which assumes the particles to be spherical (Eshel et al., 2004). Because the mutants did not grow well in K10T-1 medium, it was anticipated that the amounts of the cells were not enough for the measurements. We therefore used a prototype 200μl volume microcell for the measurements, which is not commercially available currently. The biofilm formation assays were performed with 10ml of K10T-1 in a standard 50ml centrifugal tube made of polypropylene. After static incubation at 30°C for 6h, the planktonic cells were collected by centrifugation (7.4k rpm for 2min), and the cell-free supernatants were discarded so that the residual bacterial solutions were roughly 200μl. The bacterial cells were resuspended using a micropipette, and then placed into the microcell using a disposable plastic syringe. For the measurement of biofilm cells, the 50ml tubes were washed twice with the PBS buffer, and then 10 ml of the fresh buffers were added. The biofilm cells were dispersed using an ultrasound homogenizer VC-130 equipped with a 2mm microtip (Sonics & Materials, Inc.). The amplitude was set to 20~25%. The dispersed biofilm cells were collected by centrifugation and used for the measurements as described above.

Results

Mutants incapable of *de novo* purine biosynthesis show reduced biofilm formation, but are rescued by addition of adenine and hypoxanthine. Our previous transposon mutagenesis study indicated that the genes involved in the *de novo* purine nucleotide biosynthesis are required for normal biofilm formation by *P. fluorescens* Pf0-1 (Newell et al., 2011b). To verify this, we constructed the clean deletion mutants for eight genes among total of eleven genes located in the pathway from PRPP to IMP, and examined their biofilm formation (Fig. 1A). Both PurN and PurT catalyze the same enzymatic step from 5-phosphoribosylglycinamide (GAR) to 5'-phosphoribosyl-*N*-formylglycinamide (FGAR). Since it was anticipated that the deletion of one of the genes would be compensated by the other, we did not make mutants for these genes. For the Δ*purB* mutant, we were unable to delete the gene despite repeated attempts. We therefore did not investigate these three genes in this study. As shown in Fig. 1A, biofilm formation by the mutants was reduced to less than half of that by WT, which confirms the transposon mutagenesis study.

To test whether these mutations were sufficient to explain the decrease in biofilm, we performed a complementation analysis, reintroducing each gene on a plasmid (Fig. 1B). Sufficient restoration of the biofilm formation was observed for complemented strains of Δ*purD*, Δ*purH*, Δ*purL*, Δ*purC*, and Δ*purK*. The recovery of biofilm formation was partial for complemented strains of Δ*purM*, Δ*purF*, and Δ*purE*, (Fig. 1B). An increase in arabinose concentration in the biofilm assay medium may lead to full recovery of biofilm formation, however, we did not perform further experiments.

As an alternative complementation approach, the effect of adding purine bases to the growth medium on biofilm formation by WT and three mutants, Δ*purH*, Δ*purC*, and Δ*purK*, was examined (Fig. 1C). In the salvage pathway, adenine, guanine, hypoxanthine and xanthine are converted to the corresponding nucleotides by adenine phosphoribosyltransferase and

hypoxanthine-guanine phosphoribosyltransferase and xanthine phosphoribosyltransferase. The biofilm phenotypes shown in Fig. 1C indicated that only adenine and hypoxanthine were able to recover the same level of biofilm formation as that of WT. On the other hand, addition of guanine or uric acid did not affect biofilm formation. Interestingly, xanthine and oxidized purines, isoguanine and 8-hydroxyguanine, slightly promoted biofilm formation by Δ*purH* and Δ*purK*. Incorporation of xanthine into DNA and RNA was previously reported for *E. coli* mutants that cannot convert IMP to XMP or AMP (Pang et al., 2012). A similar mechanism may work for this case. In contrast, caffeine, theobromine and theophylline that are the methylated derivatives of xanthine, were insensitive to the biofilm formation by WT, Δ*purH* and Δ*purK*. Very minor inhibitory effect was found for Δ*purC* (Fig. 1C).

One of the reasons for the reduced biofilm formation by the mutants could be a growth defect in the medium used in the assay, K10T-1. The supernatant for WT in the biofilm formation assay gradually became cloudy due to the growth of the cells. On the other hand, those for the mutants were clear and did not become turbid. To compare the growth of the cells during planktonic culture in this medium, changes in the absorbance at 600nm (OD_{600}) were monitored for WT and the above three mutants (Δ*purH*, Δ*purC*, and Δ*purK*) (Fig. 1D). It was apparent that the OD_{600} for mutants did not change during 6hrs, indicating that the mutants were not able to grow in K10T-1 medium. Addition of adenine into the medium rescued mutant growth, as the OD_{600} started to rise sharply at around 4hrs, as observed for WT (Fig 1E). This result is consistent with the recovery of the biofilm formation in the presence of adenine, as shown in Fig. 1C. It therefore seems likely that reduced biofilm formation by mutants in *de novo* purine biosynthesis pathway is due, in part, to the inability to grow in K10T-1 medium.

Purine biosynthesis mutations alter the proportion of attached verses planktonic cells in static culture. Although biofilm formation by the mutants was reduced to less than half of that by WT (Fig. 1A), it conversely

suggests that certain numbers of mutant cells were attached to the surface as biofilms. To examine this more closely, the numbers of cells in the planktonic and attached populations were determined (Fig. 2A). It is known that LB medium contains substantial amounts of nucleic acids derived from yeast extract. Therefore, it is not surprising that the mutants grew well in LB medium, which was used to culture the inoculum for the biofilm assay (black bars in Fig. 2A).

Comparing dark and light grey bars in Fig. 2A provides information on the proportion of biofilm cells versus planktonic cells, respectively. The fraction of the total cells that were attached to the surface was larger for the Δ*purC* (~69%), Δ*purK* (~75%) and Δ*purH* (~48%) mutants, compared to that for WT (~16%). These data seem to indicate that the mutants exhibit a growth defect in planktonic culture in K10T-1, and are consistent with the growth curves shown in Fig. 1D. They are also consistent with the survival of cells under purine deprivation in the biofilm mode of growth.

Secondly, it should be noted that the cell numbers of the biofilms for the Δ*purH* and Δ*purK* mutants were almost the same as that of WT. Remember that the CV staining of Δ*purH* mutant biofilms was reduced to ~40% of the WT (Fig. 1A). One explanation for the reduction in biofilm biomass by the Δ*purH* mutant could be a reduction in cell size of the Δ*purH* mutant compared to that of WT. In contrast, the cell number from the biofilm of the Δ*purC* mutant was one-order of magnitude lower than the others. Therefore, reduction in cell number should also be considered as a contributor to reduced biofilm formation by the mutants. Altogether, these observations provided a hypothesis that the reduction in biofilms by the mutants is originated from the reduction(s) in cell sizes and/or cell numbers for the biofilm cells.

Cell size is altered by purine deprivation, and by surface attachment independent of purine deprivation. From the cell counting experiments, we hypothesized that the mutant cells in biofilms became smaller than WT. To test this, SEM images for WT and the three mutants cultured in

K10T-1 were obtained (Fig. 2B). These data indicated that the mutant cells were more sparsely attached to the surface, and became smaller than the WT cells. To clarify the difference in the cell sizes between WT and the mutants, the SEM images were analyzed by measuring the circumscribed circle diameter of individual cells as an approximation for the length of the cell (described further in Materials & Methods). Shown below the SEM images in Fig. 2 are the histograms created for the each strain where the horizontal lines and vertical lines show the circumscribed diameters and the cell counts, respectively. The medians of the circumscribed circle diameter are indicated in the each histogram. The medians for the circumscribed circle diameter for the Δ*purH*, Δ*purC*, and Δ*purK* mutants were 1.31, 1.35, and 1.43μm, respectively, and became smaller than WT (1.87μm) by 25~30%.

As the impaired biofilm formation by the mutants was restored by the supplementation of adenine (Fig. 1C), we expected that the cell sizes for the mutants would return to the equivalent size of WT. Figure 2C shows the electron micrographs and histograms obtained for the adenine-supplemented biofilm cells of WT and the mutants. Against our expectation, the WT cells showed the smaller size (1.74μm) compared to that (1.87μm) in K10T-1 medium. The circumscribed circle diameters of the Δ*purH*, Δ*purC*, and Δ*purK* mutants when adenine was added to K10T-1 were 1.59, 1.70, and 1.63μm, respectively. This represents a significant increase in mutant cell size due to the addition of adenine, ranging between 14-26%, suggesting that adenine supplementation can rescue the defect in cell size shown by the mutants (Table 1).

Biofilm cells have smaller cell sizes than planktonic ones. As revealed by the SEM analyses, the biofilm cells of the mutants possess smaller cell sizes than WT. The observation seems to be similar to that happens when bacteria are placed under condition like carbon starvation (Östling et al., 1993) or undergo what are typically called reductive divisions (Roszak & Colwell, 1987; Nyström, 2004). In the latter case, cell number increases without significant increase in biomass, which accompanies decrease in the cell size

PeerJ PrePrints | https://dx.doi.org/10.7287/peerj.preprints.1307v1 | CC-BY 4.0 Open Access | rec: 13 Aug 2015, publ: 13 Aug 2015

(Roszak & Colwell, 1987; Nyström, 2004). The reason for our observation may be ascribed to survival of the mutants on the surface under the purine limitation. This is an interesting hypothesis, but has not been confirmed yet. One way to prove this is to know the sizes of the planktonic cells and compare those of the biofilm cells.

To get insights into the cell sizes for the planktonic cells, the size distributions for the planktonic cells were measured using a laser diffraction particle analyzer (Fig. 3). We compared the mode diameters that are the highest peak of the frequency distribution and represent the most commonly found particle sizes in the distributions. The coefficient of variation (COV), the normalized standard deviation through division by the mean, was also calculated to show the distribution width for each measurement: the higher the COV, the greater the dispersion in the mode diameter. The summary of the mode diameters and COVs is shown in Table 2.

Shown in Fig. 3A are the frequency distributions for the planktonic cells of WT cultured in K10T-1 (solid line) and K10T-1+adenine (dashed line). Note that the solid line almost overlapped the dashed line. The mode diameter for the cells grown in K10T-1 was 1.86μm (COV: 62.7%). The addition of adenine to K10T-1 did not change the size of the planktonic cells (1.86μm, COV: 60.4%). Biofilm cells were also analyzed after removal from the surface, which is shown in the dotted line in Fig. 3A. It is apparent that the mode diameter of the biofilm cells (1.62μm, COV: 54.7%) was smaller than that of the planktonic cells in K10T-1 (1.86μm, COV: 62.7%), suggesting that the change in life style from the planktonic to the surface-attached make the cell size smaller even for the WT cells (Table 2).

A similar reduction in cell sizes for biofilm cells occurred in the mutants (Table 2). The size distributions for the biofilm cells of the mutants are shown in the dotted line in Fig. 3B, C, and D. The mode diameters of the biofilms cells were 1.08μm for the Δ*purH* (COV: 62.7%) and Δ*purC* (COV: 61.5%) mutants and 1.22μm (COV: 59.8%) for the Δ*purK* mutant, which corresponds to 25~33% of

379 the size reductions. The results are consistent with the SEM analyses that
380 indicated 25~30% of reductions in the circumscribed circle diameters for mutant
381 biofilm cells compared to WT. On the other hand, the mode diameters of the
382 planktonic cells in K10T-1 medium were 1.86μm for the mutants (COV: Δ*purH*,
383 57.0%; Δ*purC*, 57.3%; Δ*purK*, 57.3%), which was similar to that of WT (1.86μm,
384 COV: 62.7%) (Table 2). Supplementation of adenine did not largely change the
385 cell sizes of the mutants (Δ*purH*, 1.85μm, COV: 67.2%; Δ*purC*, 1.86μm, COV:
386 59.6%; Δ*purK*, 1.85μm, COV: 63.8%), indicating that the planktonic cells of the
387 mutants maintain the same cell size irrespective of purine levels in the growth
388 medium (Table 2). In summary, the laser diffraction particle analyzer data
389 revealed that the surface-attached cells have a smaller cell size than the
390 planktonic cells.
391
392

PeerJ PrePrints | https://dx.doi.org/10.7287/peerj.preprints.1307v1 | CC-BY 4.0 Open Access | rec: 13 Aug 2015, publ: 13 Aug 2015

Discussion

In this study, we sought to determine the basis for the defects in the biofilm formation by the purine auxotrophic mutants of *P. fluorescens* Pf0-1, in which one of the genes involved in the *de novo* purine biosynthesis pathway to IMP was disrupted. We found that the attached biomass in the mutant biofilms was less than half of that in WT biofilms in K10T-1 medium (Fig. 1A). As this biosynthesis pathway is essential for most of bacteria, many studies have shown the impacts of the disruption of the genes in this biosynthesis pathway on virulence, biofilm formation and symbiosis. Our results confirm that the purine auxotrophic mutants of *P. fluorescens* Pf0-1 belong to the same category.

Judging from the fact that the biofilm formation is partially rescued by the complementation of the genes (Fig. 1B) or is completely recovered by the addition of the purine bases (Fig. 1C and E), the growth defect caused by the absence of the *de novo* purine biosynthesis should be considered the main reason for the decreased biofilm formation (Fig. 1D). However, the SEM analyses indicated that the cell lengths of the surface-attached mutant cells became smaller than that of WT by 25~30% (Fig. 2B and Table 1). This is consistent with the results by the laser diffraction particle analyses that indicated a similar size reduction (25~33%) for the mutants (Fig. 3 and Table 2), while the two methods utilize different theories to obtain the cell sizes. Therefore, our data argue that a reduction in cell size is one of the factors to explain the reduced biomass in mutant biofilms.

Reduction in the cell size of bacteria occurs when bacteria encounter nutrient deficient conditions. It is known that the many bacteria in oligotrophic environments such as soil and sea water have small cell sizes ranging between 0.4 and 0.8μm (Morita, 1993), and that some bacteria isolated from marine environment become smaller by 40~70% during starvation survival (Amy & Morita, 1983). Such a miniaturization of the cells, owing to the reductive division (Roszak & Colwell, 1987; Nyström, 2004), could be a main strategy for bacteria in the nutrient-poor environments because it increases the

surface-to-volume ratio and facilitates the cells to acquire substrates with the improved diffusion kinetics (Amy & Morita, 1983). *P. putida* KT2442 also responds to nutrient starvation by changing the cell shape and size (Givskov et al., 1994). The above examples are observed for the planktonic cells, but the similar cell size reduction was reported for *P. fluorescens* in soil and *P. syringae* on the leaves, in which the size reduction occurs for the surface-attached cells under nutrient-poor condition (van Overbeek et al., 1995; Hase et al., 1999; Monier & Lindow, 2003). Accordingly, these examples show that the size reduction is a general response to nutrient stress for both planktonic and surface-attached bacteria.

On the other hand, Steinberger et al. showed that the *P. aeruginosa* cells attached to the surface elongate in nutrient-poor condition (Steinberger et al., 2002). This is considered to be the adaptation strategy for the bacterium to maximize the surface for better absorbance of substrates (Steinberger et al., 2002). However, the elongation of the biofilm cells was also observed for the same species upon treatment of sub-inhibitory concentration of hydroxyurea that activates the SOS response by inhibiting the DNA replication (Gotoh et al., 2008). Using SEM, we obtained the similar result for *P. fluorescens* Pf0-1, in which the elongation occurred for the surface-attached WT cells in the presence of 5mM hydroxyurea (the median for the circumscribed circle diameter, 2.32μm; data not shown). Thus, the mechanism of the cell size control in the SOS response may be opposite to that in the nutrient stress.

The laser diffraction study further revealed that the biofilm cells of WT are smaller than those in the planktonic phase of the same medium (Fig. 3 and Table 2). A similar observation was reported for *Staphylococcus aureus*, in which differences in total cellular proteins and respiratory activity between surface-attached and planktonic cells were observed (Williams et al., 1999). Therefore, our observation suggests that some metabolic differences exist between the two states. In addition, the cells sizes of WT biofilms in the presence of adenine are smaller than those in its absence (Fig. 2C and Table 1).

PeerJ PrePrints | https://dx.doi.org/10.7287/peerj.preprints.1307v1 | CC-BY 4.0 Open Access | rec: 13 Aug 2015, publ: 13 Aug 2015

For the purine auxotrophic mutants, the salvage pathway is the sole way to synthesize the purine nucleotides. However, for WT, the excess purine base in the medium not only suppresses the *de novo* purine biosynthesis pathway (Houlberg & Jensen, 1983) but also may influence other metabolic pathways, leading to the observed shrinkage of the surface-attached cells. Further study using metabolomic and/or gene expression analyses is desired to identify the mechanism behind these changes.

In contrast to the surface-attached cells, the planktonic cells of the mutants remain the same cell size as WT irrespective of adenine supplementation (Fig. 3 and Table 2), indicating that the reductive division does not occur in this case. As shown in Fig. 2A, the numbers of the planktonic cells for the mutants were less than the inoculums, indicating cell death occurs for some planktonic cells that fail to adapt to the purine deficiency. The behavior of the planktonic cells of the mutants is different from those of *Vibrio* sp. and *P. putida* KT2442, in which the cell size reduction occurred for the planktonic cells soon after they were placed under carbon limitation (Amy & Morita, 1983; Östling et al., 1993; Givskov et al., 1994). This is an interesting observation as it indicates the surface-attached forms of the mutants are more suitable for survival rather than the planktonic ones under the purine shortage.

In support our observation, the previous studies indicated that the starved bacteria favor adhesion to surfaces, which is regarded as a survival strategy (Brown, Ellwood & Hunter, 1977; Dawson et al., 1981). Kjelleberg and Hermansson reported that starvation increased the degree of irreversible binding of marine bacteria to glass surfaces by changing the surface hydrophobicity and charge (Kjelleberg & Hermansson, 1984). More recent research has identified mechanisms by which bacteria modulate their surface properties in response to environmental conditions. *P. fluorescens* Pf0-1 uses a large surface protein, LapA, as adhesin, enabling the bacterium to form biofilm on both hydrophobic and hydrophilic surfaces (Hinsa et al., 2003). The amount of LapA on the surface of the bacterial cell is modified in response to internal

cues by the LapD-LapG c-di-GMP effector system (Newell et al., 2011a). The repeat region of LapA, rich in in small hydrophobic residues, is particularly important for biofilm formation, as revealed by a domain deletion experiment (Boyd et al., 2014). Other studies using an atomic force microscopy (AFM) elucidated that the repeat domain plays a main role in attachment to hydrophobic surfaces and that the unfolding of this region occurs in biofilm formation on hydrophilic surfaces (El-Kirat-Chatel et al., 2014a; El-Kirat-Chatel et al., 2014b). Therefore, it is possible to assume that the hydrophobicity of the cell surface is enhanced by the unfolding of the repeat region in LapA, facilitating the mutant cells to survive as the surface-attached forms. This is an interesting hypothesis, but should be elucidated by the future study.

Finally, we briefly discuss the cell size control in bacteria. There is a consensus that the cell size of bacteria is regulated by nutrient availability (Vadia & Levin, 2015). It was revealed that the concentration of UDP-glucose and fatty acid biosynthesis regulates the cell size, both of which depend on the nutrient status (Weart et al., 2006; Yao et al., 2012; Vadia & Levin, 2015). The recent reports indicated that the constant extension mechanism, in which a cell adds a constant volume before division, works for homeostasis of cell size (Amir, 2014; Campos et al., 2014; Iyer-Biswas et al., 2014; Taheri-Araghi et al., 2015). Under nutrient-poor condition, the constant volume becomes smaller than that in nutrient-rich condition, thus resulting shorter length for the daughter cells after the division. While the experiments were shown for the *E. coli* mutants with low glucose availability (Campos et al., 2014), a similar mechanism can apply to the purine-deficient mutants investigated in this study. The reduced cellular concentrations of ATP and GTP and/or some metabolic pathways using these nucleotides could make the constant volumes smaller, resulting in the reduced cells sizes in the mutants.

PeerJ PrePrints | https://dx.doi.org/10.7287/peerj.preprints.1307v1 | CC-BY 4.0 Open Access | rec: 13 Aug 2015, publ: 13 Aug 2015

Conclusions

This study examined purine auxotrophic mutants of *P. fluorescens* Pf0-1 to elucidate the basis of the defects they display in biofilm formation. We found that significantly more viable mutant cells attached to the surface than in the planktonic phase, indicating that the surface-attached mode of growth is suitable for survival of the mutants under the purine shortage. Using SEM and a laser diffraction particle analyzer, we demonstrated that the surface-attached mutant cells have smaller sizes than WT and that the surface-attached WT cells were smaller than the planktonic ones. The latter observation indicates that some modulation of cell size is a natural response of *P. fluorescens* to the biofilm environment. The reduction in the cell numbers in mutant biofilms could be another factor to explain the reduced biofilm formation by the mutants. Since the size reduction in bacteria occurs during carbon starvation, a similar mechanism may work to down-regulate the cell size in response to purine deprivation. The cellular concentrations of ATP and GTP or related metabolites may be involved in the cell size regulation. The data presented here provides a new view on the relationship between purine deficiency and biofilm formation.

Abbreviations

CV	crystal violet
COV	coefficient of variation
SEM	scanning electron microscopy

Acknowledgements

We thank Shingo Shimoyama, Shoko Wada, and Atsumi Ozaki (Jasco International Co., Ltd., Japan) for their assistance in obtaining and analyzing the scanning electron micrographs. We are grateful to Kyoko Mitsunari and Kazuhiro Yoshida (Horiba Ltd., Japan) for the measurements using a laser diffraction particle analyzer. We also thank Dr. George O'Toole for critical reading of the manuscript.

PeerJ PrePrints | https://dx.doi.org/10.7287/peerj.preprints.1307v1 | CC-BY 4.0 Open Access | rec: 13 Aug 2015, publ: 13 Aug 2015

References

Amir A. 2014. Cell size regulation in bacteria. *Physical Review Letters* 112:208102. DOI: 10.1103/PhysRevLett.112.208102.

Amy PS, Morita RY. 1983. Starvation-survival patterns of sixteen freshly isolated open-ocean bacteria. A*pplied and Environmental Microbiology* 45:1109-1115.

An R, Grewal PS. 2011. *purL* gene expression affects biofilm formation and symbiotic persistence of *Photorhabdus temperata* in the nematode *Heterorhabditis bacteriophora*. *Microbiology* 157:2595-2603. DOI: 10.1099/mic.0.048959-0.

Bacon GA, Burrows TW, Yates M. 1951. The effects of biochemical mutation on the virulence of *Bacterium typhosum*: The loss of virulence of certain mutants. *British Journal of Experimental Pathology* 32:85-96.

Boyd CD, Smith TJ, El-Kirat-Chatel S, Newell PD, Dufrêne YF, O'Toole GA. 2014. Structural features of the *Pseudomonas fluorescens* biofilm adhesion LapA required for LapG-dependent cleavage, biofilm formation, and cell surface localization. *Journal of Bacteriology* 196:2775-2788. DOI: 10.1128/JB.01629-14.

Brown, CM, Ellwood, DC, Hunter JR. 1977. Growth of bacteria at surfaces: influence of nutrient limitation. *FEMS Microbiology Letters* 1:163-166.

Campos M, Surovtsev IV, Kato S, Paintdakhi A, Beltran B, Ebmeier S, Jacobs-Wagner C. 2014. A constant size extension drives bacterial cell size homeostasis. *Cell* 159:1433-1446. DOI: 10.1016/j.cell.2014.11.022.

576 Christen, M, Christen B, Folcher M, Schauerte A, Jenal U. 2005. Identification
577 and characterization of a cyclic di-GMP-specific phosphodiesterase and its
578 allosteric control by GTP. *Journal of Biological Chemistry* 280:30829-30837.
579 DOI: 10.1074/jbc.M504429200.
580
581 Dawson MP, Humphrey BA, Marshall KC. 1981. Adhesion: A tactic in the
582 survival strategy of a marine vibrio during starvation. *Current Microbiology*
583 6:195-199.
584
585 El-Kirat-Chatel S, Beaussart A, Boyd CD, O'Toole GA, Dufrêne YF. 2014a.
586 Single-cell and single molecule analysis deciphers the localization, adhesion,
587 and mechanics of the biofilm adhesin LapA. *ACS Chemical Biology* 9:485-494.
588 DOI: 10.1021/cb400794e.
589
590 El-Kirat-Chatel S, Boyd CD, O'Toole GA, Dufrêne YF. 2014b. Single-molecule
591 analysis of *Pseudomonas fluorescens* footprints. *ACS Nano* 9:485-494. DOI:
592 10.1021/nn4060489.
593
594 Eshel G, Levy GJ, Mingelgrin U, Singer MJ. 2004. Critical evaluation of use of
595 laser diffraction for particle-size distribution analysis. *Soil Science Society of*
596 *America Journal* 68:736-743. DOI: 10.2136/sssaj2004.0736.
597
598 Ge X, Kitten T, Chen Z, Lee SP, Munro CL, Xu P. 2008. Identification of
599 *Streptococcus sanguinis* genes required for biofilm formation and examination
600 of their role in endocarditis virulence. *Infection and Immunity* 76: 2551-2559.
601 DOI: 10.1128/IAI.00338-08.
602
603 Gerber ED, Hackett AJ, Franklin R. 1952. The virulence of biochemical
604 mutants of *Klebsiella pneumoniae*. *Genetics* 38:693-697.
605

606 Givskov M, Eberl L, Møller S, Poulsen LK, Molin S. 1994. Responses to nutrient
607 starvation in *Pseudomonas putida* KT2442: Analysis of general cross-protection,
608 cell shape, and macromolecular content. *Journal of Bacteriology* 176:7-14.
609
610 Gotoh H, Zhang Y, Dallo SF, Hong S, Kasaraneni N, Weitao T. 2008.
611 *Pseudomonas aeruginosa*, under DNA replication inhibition, tends to form
612 biofilms via Arr. *Research in Microbiology* 159:294-302. DOI:
613 10.1016/j.resmic.2008.02.002.
614
615 Haas D, Defago G. 2005. Biological control of soil-borne pathogens by
616 fluorescent pseudomonads. *Nature Reviews Microbiology* 3:307-319. DOI:
617 10.1038/nrmicro1129.
618
619 Han SH, Anderson AJ, Yang KY, Cho BH, Kim KY, Lee MC, Kim YH, Kim YC.
620 2006. Multiple determinatns influence root colonization and induction of
621 induced systemic resistance by *Pseudomonas chlororaphis* O6. *Molecular Plant*
622 *Pathology* 7:463-472. DOI: 10.1111/J.1364-3703.2006.00352.X.
623
624 Hase C, Mascher F, Moënne-Loccoz, Y, Défago G. 1999. Nutrient deprivation
625 and the subsequent survival of biocontrol *Pseudomonas fluorescens* CHA0 in
626 soil. *Soil Biology and Biochemistry* 31:1181-1188. DOI:
627 10.1016/S0038-0717(99)00036-X.
628
629 Hinsa SM, Espinosa-Urgel M, Ramos JL, O'Toole GA. 2003. Transition from
630 reversible to irreversible attachment during biofilm formation by *Pseudomonas*
631 *fluorescens* WCS365 requires an ABC transporter and a large secreted protein.
632 *Molecular Microbiology* 49:905-918. DOI: 10.1046/j.1365-2958.2003.03615.x.
633
634 Houlberg U, Jensen KF. 1983. Role of hypoxanthine and guanine in regulation
635 of *Salmonella typhimurium pur* gene expression. *Journal of Bacteriology*

PeerJ PrePrints | https://dx.doi.org/10.7287/peerj.preprints.1307v1 | CC-BY 4.0 Open Access | rec: 13 Aug 2015, publ: 13 Aug 2015

153:837-845.

Humphrey B, Kjelleberg S, Marshall KC. 1983. Responses of marine bacteria under starvation conditions at solid-water interface. A*pplied and Environmental Microbiology* 45:43-47.

Iyer-Biswas S, Wright CS, Henry JT, Lo K, Burov S, Lin Y, Crooks GE, Crosson S, Dinner AR, Scherer NF. 2014. Scaling laws governing stochastic growth and division of single bacterial cells. *Proceedings of National Academy of Sciences in the USA* 111:15912-15917. DOI: 10.1073/pnas.1403232111.

Jenkins A, Cote C, Twenhafel N, Merkel T, Bozue J, Welkos S. 2011. Role of purine biosynthesis in *Bacillus anthracis* pathogenesis and virulence. *Infection and Immunity* 79:153-166. DOI: 10.1128/IAI.00925-10.

Kim JK, Jang HA, Won YJ, Kikuchi Y, Han SH, Kim C-H, Nikoh N, Fukatsu T, Lee BL. 2014a. Purine biosynthesis-deficient *Burkholderia* mutants are incapable of symbiotic accommodation in the stinkbug. *The ISME Journal* 8:552-563. DOI: 10.1038/ismej.2013.168.

Kim JK, Kwon JY, Kim SK, Han SH, Won YJ, Lee JH, Kim C-H, Fukatsu T, Lee BL. 2014b. Purine biosynthesis, biofilm formation, and persistence of an insect-microbe gut symbiosis. A*pplied and Environmental Microbiology* 80:4374-4382. DOI: 10.1128/AEM.00739-14.

Kjelleberg S, Hermansson M. 1984. Starvation-induced effects on bacterial surface characteristics. *Applied and Environmental Microbiology* 48:497-503.

Monds RD, Newell PD, Gross RH, O'Toole GA. 2007. Phosphate-dependent modulation of c-di-GMP levels regulates *Pseudomonas fluorescens* Pf0-1 biofilm

PeerJ PrePrints | https://dx.doi.org/10.7287/peerj.preprints.1307v1 | CC-BY 4.0 Open Access | rec: 13 Aug 2015, publ: 13 Aug 2015

formation by controlling secretion of the adhesion LapA. *Molecular Microbiology* 63:659-679. DOI: 10.1111/j.1365-2958.2006.05539.x.

Monds RD. Newell PD. Schwartzman JA. O'Toole GA. 2006. Conservation of the Pho regulon in *Pseudomonas fluorescens* Pf0-1. A*pplied and Environmental Microbiology* 72:19190-1924. DOI: 10.1128/AEM.72.3.1910–1924.2006.

Monds RD, Newell PD, Wagner JC, Schwartzman JA, Lu W, Rabinowitz, JD, O'Toole GA. 2010. Di-adeonosine tetraphosphate (Ap4A) metabolism impacts biofilm formation by *Pseudomonas fluorescens* via modulation of c-di-GMP-dependent pathway. *Journal of Bacteriology* 192:3011-3023. DOI: 10.1128/JB.01571-09.

Monier J-M, Lindow SE. 2003. *Pseudomonas syringae* responds to the environment on leaves by cell size reduction. *Phytopathology* 93:1209-1216.

Morita, RY. 1993. Bioavailability of energy and the starvation state. In: Kjelleberg S, ed. *Starvation in Bacteria*. New York: Plenum Press, 1-23.

Neuhard J. and Nygaar P. 1987. Purines and Pyrimidines. In: Neidhardt FC, ed. *Escherichia coli and Salmonella typhimurium Cellular and molecular biology*. Washington, D.C: American Society for Microbiology. 445-473.

Newell PD, Boyd CD, Sondermann H, O'Toole GA. 2011a. A c-di-GMP effector system controls cell adhesion by inside-out signaling and surface protein cleavage. *PLoS Biology* 9:e1000587. DOI: 10.1371/journal.pbio.1000587.

Newell PD, Monds RD, O'Toole GA. 2009. LapD is a bis-(3', 5')-cyclic GMP binding protein that regulates surface attachment by *Pseudomonas fluorescens* Pf0-1. *Proceedings of National Academy of Sciences in the USA* 106:3461-3466.

PeerJ PrePrints | https://dx.doi.org/10.7287/peerj.preprints.1307v1 | CC-BY 4.0 Open Access | rec: 13 Aug 2015, publ: 13 Aug 2015

DOI: 10.1073/pnas.0808933106.

Newell PD, Yoshioka S, Hvorecny KL, Monds RD, O'Toole GA. 2011b. Systematic analysis of diguanylate cyclases that promote biofilm formation by *Pseudomonas fluorescens* Pf0-1. *Journal of Bacteriology* 193:4685-4698. DOI: 10.1128/JB.05483-11.

Nyström T. 2004. Stationary-phase physiology. *Annual Review of Microbiology* 58:161-181. DOI: 10.1146/annurev.micro.58.030603.123818.

Östling J, Holmquist L, Flärdh K, Svenblad B, Jouper-Jaan Å, Kjelleberg S. 1993. Starvation and Recovery of Vibrio. In: Kjelleberg S, ed. *Starvation in Bacteria*. New York: Plenum Press, 103-127.

Pang B, McFaline JL, Burgis NE, Dong M, Taghizadeh K, Sullivan MR, Elmquist CE, Cunningham RP, Dedon PC. 2012. Defects in purine nucleotide metabolism lead to substantial incorporation of xanthine and hypoxanthine into DNA and RNA. *Proceedings of National Academy of Sciences in the USA* 109:2319-2324. DOI: 10.1073/pnas.1118455109.

Paul R, Weiser S, Amiot NC, Chan C, Schimer T, Giese B, Jenal U. 2004. Cell cycle-dependent dynamic localization of a bacterial response regulator with a novel di-guanylate cyclase output domain. *Genes & Development* 18:715-727. DOI: 10.1101/gad.289504.

Pilatz S, Breitbach K, Hein N, Fehlhaber B, Schulze J, Brenneke B, Eberl L, Steinmetz I. 2006. Identification of *Burkholderia pseudomallei* genes required for the intracellular life cycle and in vivo virulence. *Infection and Immunity* 74:3576-3586. DOI: 10.1128/IAI.01262-05.

726 Polissi A, Pontiggia A, Feger G, Altieri M, Mottl H, Ferrari L, Simon D. 1998.
727 Large-scale identification of virulence genes from *Streptococcus pneumoniae*.
728 *Infection and Immunity* 66:5620-5629.
729
730 Roszak DB, Colwell RR. 1987. Survival strategies of bacteria in the natural
731 environment. *Microbiological Reviews* 51:365-379.
732
733 Ryan RP, Fouhy Y, Lucey JF, Crossman LC, Spiro S, He Y-W, Zhang L-H, Heeb
734 S, Cámara M, Williams P, Dow JM. 2006. Cell-cell signaling in *Xanthomonas*
735 *campestris* involves an HD-GYP domain protein that functions in cyclic di-GMP
736 turnover. *Proceedings of National Academy of Sciences in the USA*
737 103:6712-6717. DOI: 10.1073/pnas.0600345103.
738
739 Ryjenkov DA, Tarutina M, Moskvin OV, Gomelsky M. 2005. Cyclic diguanylate
740 is a ubiquitous signaling molecule in bacteria: insight into biochemistry of the
741 GGDEF protein domain. *Journal of Bacteriology* 187:1792-1798. DOI:
742 10.1128/JB.187.5.1792-1798.2005.
743
744 Samant S, Lee H, Ghassemi M, Chen J, Cook JL, Mankin AS, Neyfakh AA.
745 2008. Nucleotide biosynthesis is critical for growth of bacteria in human blood.
746 *PLoS Pathogens* 4:e37. DOI: 10.1371/journal.ppat.0040037.
747
748 Schmidt, AJ, Ryjenkov DA, Gomelsky M. 2005. The ubiquitous protein domain
749 EAL is a cyclic diguanylate-specific phosphodiesterase: enzymatically active
750 and inactive EAL domains. *Journal of Bacteriology* 187:4774-4781. DOI:
751 10.1128/JB.187.14.4774-4781.2005.
752
753 Shanks RM, Caiazaa NC, Hinsa SM, Toutain CM, O'Toole GA. 2006.
754 *Saccharomyces cerevisiae*-based molecular tool kit for manipulation of genes
755 from gram-negative bacteria. A*pplied and Environmental Microbiology*

PeerJ PrePrints | https://dx.doi.org/10.7287/peerj.preprints.1307v1 | CC-BY 4.0 Open Access | rec: 13 Aug 2015, publ: 13 Aug 2015

72:5027-5036. DOI: 10.1128/AEM.00682-06.

Shimada K, Itoh Y, Washio K, Morikawa M. 2012. Efficacy of forming biofilms by naphthalene degrading *Pseudomonas stutzeri* T102 toward bioremediation technology and its molecular mechanisms. *Chemosphere* 87:226-233. DOI: 10.1016/j.chemosphere.2011.12.078.

Steinberger RE, Allen AR, Hansma HG, Holden PA. 2002. Elongation correlates with nutrient deprivation in *Pseudomonas aeruginosa*-unsaturated biofilms. *Microbial Ecology* 43:416-424. DOI: 10.1007/s00248-001-1063-z.

Straley AC, Harmon PA. 1984. Growth in mouse peritoneal macrophages of *Yersinia pestis* lacking established virulence determinants. *Infection and Immunity* 45:649-654.

Taheri-Araghi S, Bradde S, Sauls JT, Hill NS, Levin PA, Paulsson J, Vergassola M, Jun S. 2015. Cell-size control and homeostasis in bacteria. *Current Biology* 25:385-391. DOI: 10.1016/j.cub.2014.12.009.

Vadia S, Levin PA. 2015. Growth rate and cell size: a re-examination of the growth law. *Current Opinion in Microbiology* 24:96-103. DOI: 10.16/j.mib.2015.01.011.

Van Overbeek LS, Eberl L, Givskov M, Molin S, van Elsas JD. 1995. Survival of, and induced stress resistance in, carbon-starved *Pseudomonas fluorescens* cells residing in soil. *Applied and Environmental Microbiology* 61:4202-4208.

Wang J, Mushegian A, Lory S, Jin S. 1996. Large-scale isolation of candidate virulence genes of *Pseumonas aeruginosa* by in vivo selection. *Proceedings of National Academy of Sciences in the USA* 93:10434-10439.

PeerJ PrePrints | https://dx.doi.org/10.7287/peerj.preprints.1307v1 | CC-BY 4.0 Open Access | rec: 13 Aug 2015, publ: 13 Aug 2015

786
787 Weart RB, Lee AH, Chien AC, Haeusser DP, Hill NS, Levin PA. 2007. A
788 metabolic sensor governing cell size in bacteria. *Cell* 130:335-347. DOI:
789 10.1016/j.cell.2007.05.043.
790
791 Williams I, Paul F, Lloyd D, Jepras R, Critchley I, Newman M, Warrack J,
792 Giokarini T, Hayes AJ, Randerson PF, Venables WA. 1999. Flow cytometry and
793 other techniques show that *Staphylococcus aureus* undergoes significant
794 physiological changes in the early stages of surface-attached culture.
795 *Microbiology* 145:1325-1333.
796
797 Yao Z, Davis RM, Kishony R, Kahne D, Ruiz N. 2012. Regulation of cell size in
798 response to nutrient availability by fatty acid biosynthesis in *Escherichia coli*.
799 *Proceedings of National Academy of Sciences in the USA* 109:E2561-E2568.
800 DOI: 10.1073/pnas.1209742109.
801
802 Yousef F & Espinosa-Urgel M. 2007. *In silico* analysis of large microbial surface
803 proteins. *Research in Microbiology* 158:545-550. DOI:
804 10.1016/j.resmic.2007.04.006.

Figure 1(on next page)

Effect of the mutation of the genes in the de novo *purine nucleotide biosynthesis on biofilm formation and growth.*

(A) A quantitative biofilm assay comparing WT and the clean deletion mutants. Data are the mean absorbance of dissolved crystal violet stained biomass at 550nm ± standard deviations (SD) (n = 7). Representative images for the biofilms are shown above the graphs. (B) A quantitative biofilm assay to examine complementation of the genes for the clean deletion mutants (gray bars). The pMQ72 vector with each gene was introduced into the parent strain. The WT strain contained an empty pMQ72 vector. Arabinose was added to the medium at a concentration of 0.1% to induce the gene expression. Strains without the pMQ72 vector are shown in black bars as references. Data are the mean absorbance at 550 nm ± SD (n = 7). Representative images for the biofilms with the gene complementation are shown above the graphs. (C) A quantitative biofilm assay for WT (black), ΔpurH (gray), ΔpurC (light gray), and ΔpurK (white) in the presence of various purine bases. Data are the mean absorbance at 550 nm ± SD (n = 8). Asterisks (*) show a statistically significant difference in absorbance relative to the medium without exogenous purines ($P < 0.01$ in two-tailed Student's t-test assuming equal variance). Each purine base was added to the medium at concentration of 0.2mM. (D) Time-dependent change in cell density for WT (◆) and the mutants (ΔpurH (▲), ΔpurC (●) and ΔpurK (■)) in K10T-1 medium (absorbance at 600nm; mean ± SD, n = 8). The experiment was performed in the same volume as the biofilm formation assay. (E) Time-dependent change in cell density for WT (◆) and the mutants (ΔpurH (▲), ΔpurC (●) and ΔpurK (■)) when 1mM adenine was added to the medium (absorbance at 600nm; mean ± SD, n = 8).

Figure 1

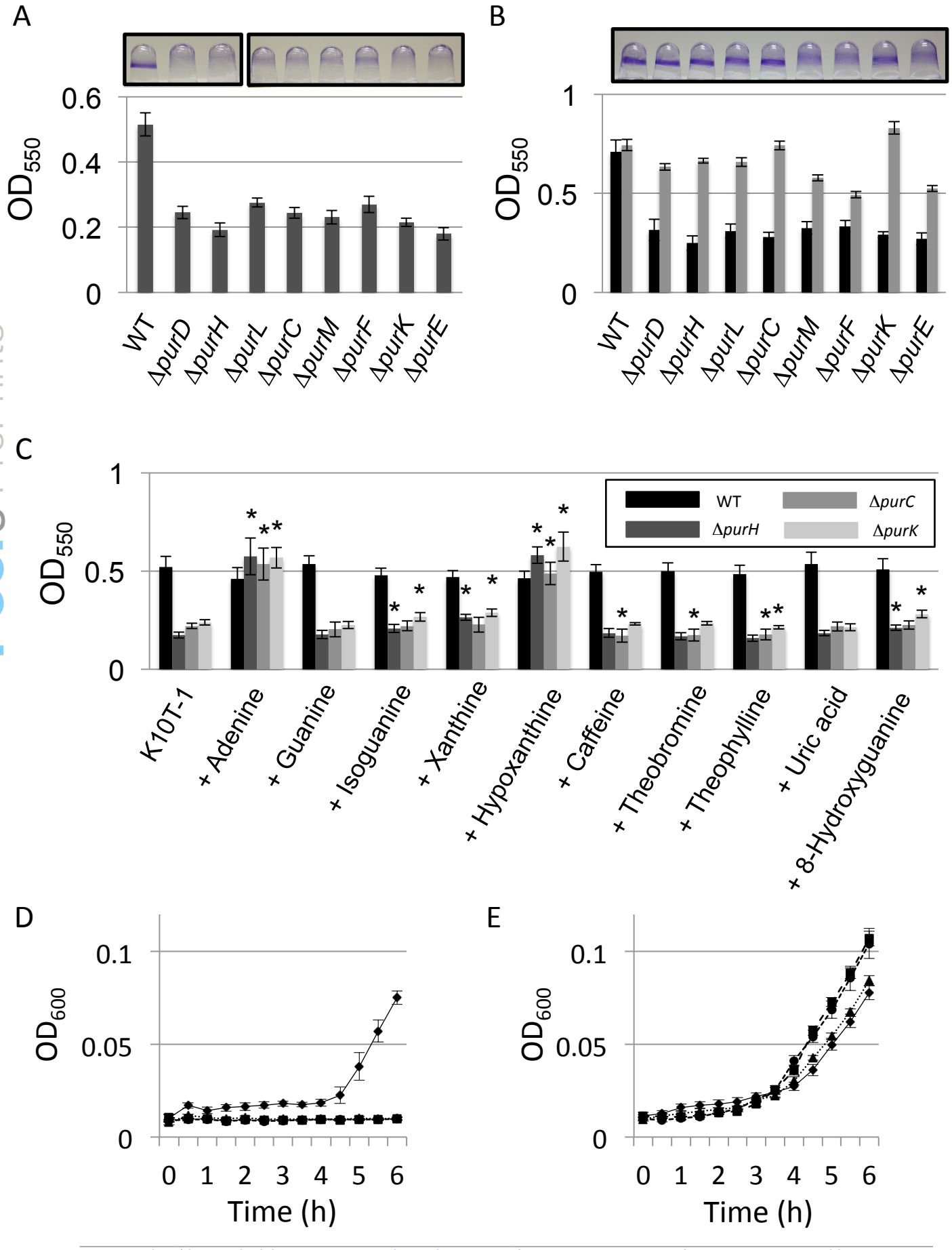

Figure 2(on next page)

Effect of the mutations on numbers and sizes of the cells in biofilms.

(A) The black, dark gray, and light gray bars indicate number of the cells in the inoculum (t=0hrs), biofilms (t=6hrs), and supernatants (t=6hrs), respectively, for WT and the three mutants (ΔpurH, ΔpurC and ΔpurC); mean ± SD, n = 4. (B) Scanning electron micrographs showing the differences in cell size of the biofilm cells between WT and the mutants (ΔpurH, ΔpurC and ΔpurC). The white bars represent 5µm. The histograms shown below the micrographs are the output data from the Phenom ParticleMetric software shown with minor modifications on the axes and labels for clarity. The medians of the circumscribed circle diameters are indicated on the each histogram. (C) Scanning electron micrographs showing changes in the cell sizes upon supplementation of 0.2mM adenine into the medium. The white bars indicate 5µm. The histograms labeled with the medians are shown below the micrographs.

Figure 2

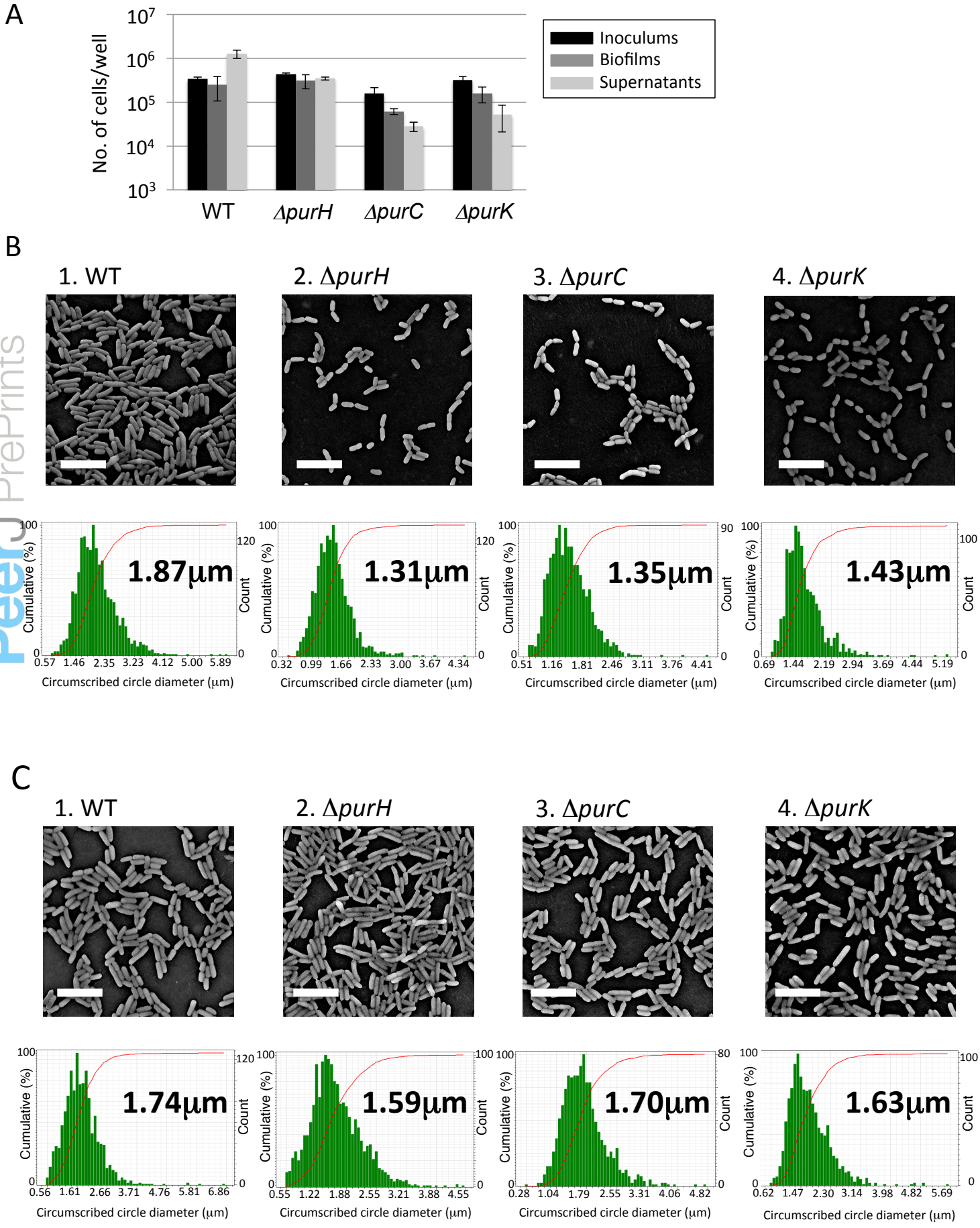

Figure 3(on next page)

The size distributions for the planktonic and biofilm cells of WT and mutants obtained using a laser diffraction particle analyzer.

Panel A, B, C, and D show the size distribution for WT, ΔpurH, ΔpurC, and ΔpurK, respectively. For each panel, the size distributions for planktonic and biofilm cells cultured in K10T-1 medium are shown in solid and dotted lines, respectively. The dashed lines indicate the size distributions for the planktonic cells cultured in the medium with 0.2mM adenine.

Figure 3

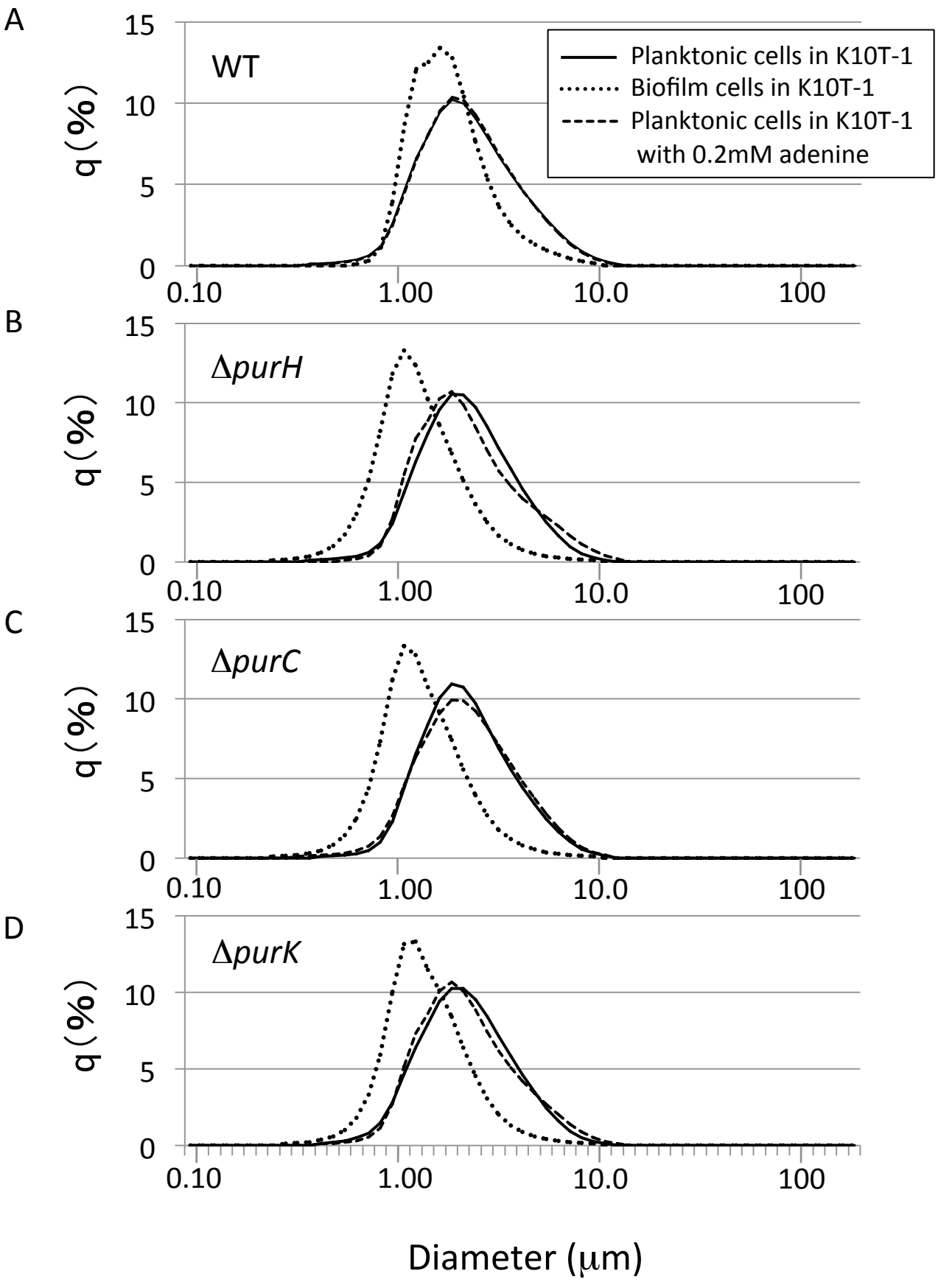

Table 1 (on next page)

Summary of the circumscribed circle diameters (μm) for WT and the mutants obtained by the SEM analyses.

The parentheses indicate the *P* values obtained by the Wilcoxon Sum Rank test. [a] *P* value when compared to the WT values in the same media. [b] *P* value when compared to the same strain in K10T-1 medium. [*] The asterisk indicates no statistically significant difference in size relative to that of WT in the same medium ($P > 0.05$).

Table. 1. Summary of the circumscribed circle diameters (μm) for WT and the mutants obtained by the SEM analyses.

	WT	Δ*purH*	Δ*purC*	Δ*purK*
K10T-1	1.87	1.31	1.35	1.43
		(< 2.2E-16)[a]	(< 2.2E-16)[a]	(< 2.2E-16)[a]
+ 0.2mM adenine	1.74	1.59	1.70	1.63
		(3.02E-09)[a]	(0.05198)[a, *]	(0.0002705)[a]
	(8.27E-14)[b]	(< 2.2E-16)[b]	(< 2.2E-16)[b]	(< 2.2E-16)[b]

The parentheses indicate the *P* values obtained by the Wilcoxon Sum Rank test.

[a] *P* value when compared to the WT values in the same media.

[b] *P* value when compared to the same strain in K10T-1 medium.

[*] The asterisk indicates no statistically significant difference in size relative to that of WT in the same medium ($P > 0.05$).

Table 2 (on next page)

Summary of the mode diameters (μm) for the planktonic and biofilm cells of WT and the mutants obtained by a laser diffraction particle analyzer.

Summary of the mode diameters (μm) for the planktonic and biofilm cells of WT and the mutants obtained by a laser diffraction particle analyzer.

Table 2. Summary of the mode diameters (μm) for the planktonic and biofilm cells of WT and the mutants obtained by a laser diffraction particle analyzer.

	WT	Δ*purH*	Δ*purC*	Δ*purK*
Planktonic cells in K10T-1	1.86 (62.7)	1.86 (57.0)	1.86 (57.3)	1.86 (57.3)
Planktonic cells in K10T-1 + 0.2mM adenine	1.86 (60.4)	1.85 (67.2)	1.86 (59.6)	1.85 (63.8)
Biofilm cells in K10T-1	1.62 (54.7)	1.08 (62.7)	1.08 (61.5)	1.22 (59.8)

The parentheses indicate the coefficient of variations (COV) expressed as percentage (%).